



*Course Title: **Robot Design and Experimentation***

*Project Title: **Oswald***

*Report Title: **Final Project Report***

*Group: **9***

*Angelos Mavrogiannis  
Pranav Narahari  
Stam Athinotis*

*William Moreno  
Aniruddhan Unni*

## Abstract

The ocean has been a pivotal aspect of human life and researchers throughout the world have recently focused their attention on mapping earth's seafloor and gaining a more complete insight of the ocean's ecosystem. Acknowledging the monumental aspect of such an endeavor, the research community has turned to robotics for collection of an enormous amount of data to enhance our understanding by exploiting less human power. This project intends to offer stronger insights into alternative forms of locomotion for niche uses by designing and testing a bio-inspired robot which utilizes penguins' principal propulsion mechanism and unique body shape. The objective was to study and optimize the effects of flipper shape, flexibility, and length through underwater tests at Carnegie Mellon's Field Robotics Center. However, simulations informed many design choices and allowed for an understanding of effect the flipper shape and length wherein tapered and swept/curved flippers allow for a smaller tip vortex thereby reducing the associated induced drag.

## Introduction

In 2013, the Schmidt Ocean Institute and NASA reported that only 5-15% of the Earth's ocean floor has been properly mapped [1]. This leads to the surprising conclusion that we know more details about the surface of Mars than earth's seafloor with current resolution of obtained mappings being 20 meters and 5 kilometers respectively [2]. These findings urged the marine research community to allocate resources and funds in designing and building robots that would accelerate and optimize the process of collecting continuous data by minimally invading the ecosystem. This requires energy-efficient propulsion methods that may lie outside the spectrum of conventional propeller designs.

Propulsion and maneuvering underwater by flapping foil motion, optimized through years of evolution, is ubiquitous in nature, yet marine propulsors inspired by examples of highly maneuverable marine life are not widely implemented in engineering. The use of biomimetic tandem flapping foils for underwater vehicles is considered as a unique and interesting concept in the area of marine propulsion. The flapping wings can be used as thrust producing, stabilizing and control devices which have both propulsion and maneuvering applications for marine vehicles [3]. Additionally, the outer shape of marine animals and vehicles play a pivotal role in both the overall efficiency and maximum achievable speed. A streamlined body significantly enhances their performance by minimizing the drag and allowing them to attain higher velocities with lower cost of transportation [4]. Thus, flippers, together with a hydrodynamic body shape, allow penguins to achieve high speeds and maneuverability, while maintaining low energy consumption levels. Hence, they are rightfully regarded as one of the most efficient marine animals, as illustrated in Figure 1.

Researchers and engineers have long been interested in the flapping motion of birds as a means of propulsion. Existing robots that draw inspiration from birds have focused on mimicking their flight behavior, like Clear Flight Solutions' Robird [5]. These robots are using their resemblance to other birds by successfully blending in with them and offering interesting solutions to applications such as airport bird control, surveillance or agriculture. While the existing research has been focusing mainly on the flapping motion of birds for aerial robotics, there hasn't been extensive work on flapping motion underwater, specifically targeted towards underwater robotics.



**Figure 1: Penguins diving underwater (photo credit: National Geographic Magazine, Paul Necklen)**

There have been some attempts to reproduce the flapping motion of marine animals underwater, such as the MantaDroid [6], an aquatic robot that emulates the swimming locomotion of manta rays, developed by researchers from the National University of Singapore. The most relevant robotic application in this area is Festo's AquaPenguin [7], an autonomous underwater robot that imitates a penguin, both visually and kinematically. Using a 3D sonar for perception, an electric motor for the flapping motion and an actuator for each of its wings to control the roll, the AquaPenguin can navigate autonomously, replicating the penguins' behavior. Even though the AquaPenguin does a decent job replicating the motion of penguins, there is significant potential for improvement in the flapping motion to approach the performance of an actual penguin. Moreover, the flapping motion or flipper design has not been characterized in a way that is conducive to further research and there are still significant questions that are yet to be answered.

The effect of the shape parameters of a flipper for example, haven't been characterized nearly as much as airplane wings or propellers. The effect of the flexibility of oscillating foil propellers for ships have been studied for some cases [8] but this effect still hasn't been analysed or quantified for flapping foil motion.

## Research Question

Taking into consideration the motives that encouraged our team to proceed in designing and fabricating a penguin-inspired robot, along with the work that has been completed so far in the field of ocean explorations and exploited underwater vessels, the research hypothesis that we propose, and expect to answer with our functional prototype is: *“How does the design of the flipper, namely its length (aspect ratio), curvature (or sweep) and flex (or compliance) affect the speed and energy efficiency of penguins swimming underwater”*.

## Final Design

After many iterations, the final design of the robot consists of a 2 DoF flapping mechanism that is powered by a DC motor to manage the frequency of flapping and 2 servo motors on the flippers to control their angle of attack. The electronics are housed in an internal waterproof box behind the mechanism and the entire assembly is covered by an outer body that consists of a rib and spar design with a heat-sealed Polyurethane coating and rubber covering for additional waterproofing.

## Flapping Mechanism & Ball Joint

Admittedly, one of the most crucial components of our robot is the mechanism that enables the flapping motion to reach the desired angle range and speed along with all target specifications regarding the controlled degrees of freedom and efficiency. Therefore, right from the beginning, the team was focused on designing an analogous mechanism that would provide the required functionalities. Three designs capable of converting rotational motion of the motor into flapping motion were developed. The first mechanism was inspired by the wiper mechanism used in commercial vehicles for windshield cleaning [See appendix A2]. The major drawback of this mechanism was the limited flapping range which led to the development of the next two designs. The second concept was inspired by flapping mechanisms currently utilized in robotic birds. The mechanism overcame the problem of limited range but posed a new issue of sealing the joint due to the addition of a sliding pivot point [See appendix A3]. The final mechanism was realised with the addition of a ball-and-socket joint as the pivot point of the wing (Figure 2). Despite the difficult manufacturability, the ball-and-socket joint was chosen for its ability to transmit motion in all directions. The addition of the ball-and-socket joint would also make it easy to add a third degree of freedom to the wing with ease. The most suitable mechanism was selected based on the performance comparison of the three models explained above. The key parameters for comparison were the flapping range (angle swept in one complete flapping cycle) and the angular acceleration of the tip of the flipper (to determine the output torque of the model). The Kinematic Analysis was carried out on SolidWorks using the SolidWorks Motion Analysis package.

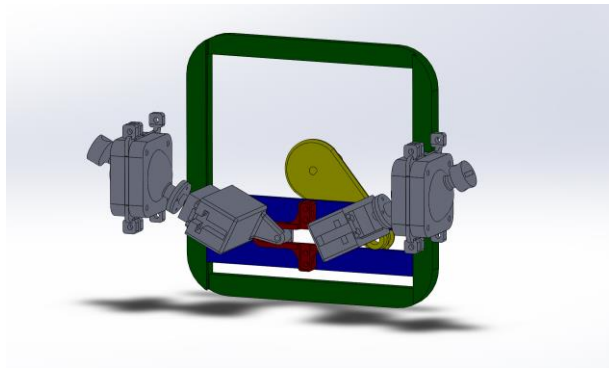


**Figure 2: Final Mechanism**

### Kinematic, Dynamic and Control model

For the kinematic model of our robot, the flapping wing has two distinct motions [9]: a) Rolling motion or flapping motion ( $\theta_1$ ), which is the up and down plunging motion of the wing. Flapping produces the majority of the robot's power and has the largest range of motion b) Pitching motion ( $\theta_2$ ) of the wing determines the final angle of attack between the resultant water velocity and the horizontal of the flipper. The dynamic model of the robot was developed by assuming the robot is a set of 3 rigid bodies, with one body allocated for the fuselage and one for each wing (Figure-3). Each wing is connected to the body by means of a revolute joint (roll) and a rotary joint (pitch). Applying forward kinematics on this model results in the final wing orientation, and hence the wing velocity with respect to the body. This velocity is also known as the heave velocity, [See appendix A4] which is used to calculate the instantaneous angle of attack. Using the angle of attack and the hydrodynamics of the wing [See appendix A5], the forward velocity of the robot is calculated. This forward velocity is used as a feedback to a PID [10] controller which varies the input rpm of the motor to achieve the desired forward velocity (Figure-4).

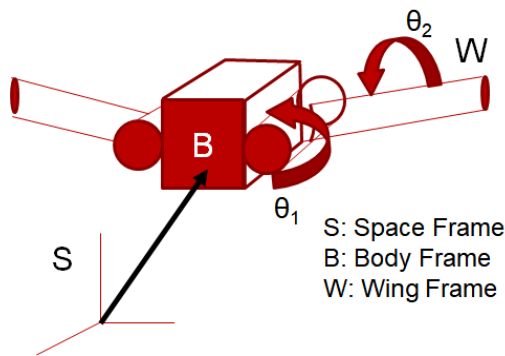


**Figure 3: Dynamic model**

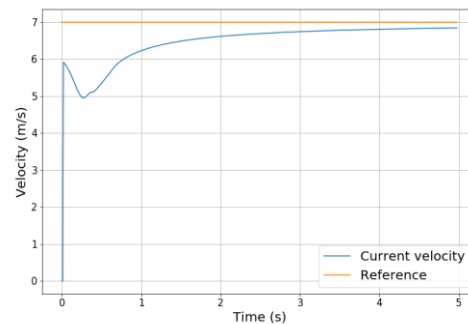


**Figure 4: PID controller feedback**

### Body and Flipper Design

As mentioned earlier, the two key features that allow penguins to achieve their remarkable maneuverability and speed underwater are their streamlined body shape and flippers. CFD or Computational Fluid Dynamics Simulations were used in order to optimize both the features and characterize the forces/moments acting on the penguin in order to aid motor selection, kinematics and stability controls.

The body shape was constrained primarily by the size of the internal mechanism which sits in the middle of the robot. Given the size constraints, the objective was to minimize the coefficient of drag whilst keeping the size and shape in such a manner that it can be manufactured easily using the equipment/materials available. An iterative design process was followed by starting with a teardrop shape (which is known to have a very low coefficient of drag) and iterating towards the shape of an actual penguin. 2D axisymmetric simulations were carried out in ANSYS Fluent 19 R1 initially, followed by full scale 3D steady-state simulations. The Reynold's number was approximately of 1 to 2,000,000 (making the flow fully turbulent). As a result, the Reynolds Averaged Navier Stokes (RANS) Equations were used along with the 2-equation realizable kE turbulence model [See appendix B.1]. These settings along with the mesh size were determined using a thorough convergence study [See appendix B.2]. The final coefficient of drag was reduced from 0.81 to 0.54 and the design couldn't be optimized further without significantly

hindering the manufacturing. Given that the actual Coefficient of drag of the most efficient penguin species is close to 0.02 [11], the design was deemed sufficient.

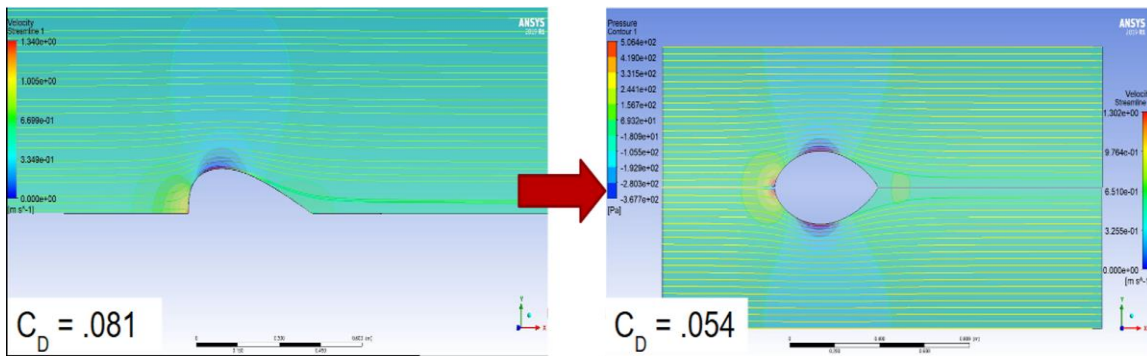


Figure 5: Velocity streamlines and pressure contours for the initial and final body design

The second crucial aspect that had to be optimized hydrodynamically was the design of the flipper. Images of the gentoo penguins (which are the closest species in size to our robot) at the Pittsburgh zoo were used to get a baseline design for the flipper. The lift and drag were calculated for every angle of attack for the flipper in order to generate the thrust and drag profile. 3D steady state simulations were performed on ANSYS Fluent 19 R1 using the RANS equations and the  $k-\omega$  2 equation turbulence model. The mesh and physics settings were obtained after running a 5 stage convergence study as before. The lift and drag polars [See appendix B.3] were obtained and this data was used for motor selection, optimizing the flapping controls and improving on the base design.

Based on the research hypothesis, three elements of flipper design were to be examined- the length or aspect ratio, the sweep or curvature and the flex or compliance. In order to do this systematically, two to three flippers were designed to test each aspect separately. Firstly, longer and narrower flippers with a higher aspect ratio (from 5:1 for the base case to 7.5:1 for the most slender wing) were created to study the possible increase in efficiency versus the structural tradeoff of doing this. Secondly, two additional flippers with increasing degrees of curvature or wing sweep were designed to test the effect of the shape. Lastly, all the flippers were made again using thinner material that flexes more in order to study that effect. The flippers were designed in such a way that the center of pressure always rests on the axis on which the flippers move up and down.

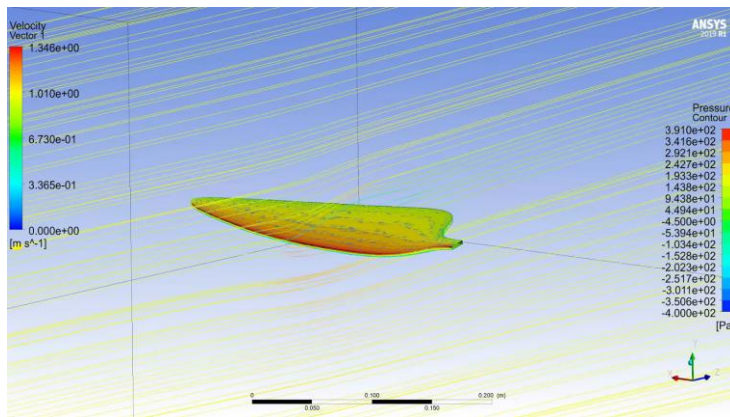


Figure 6: Isometric view of the flipper with velocity streamlines

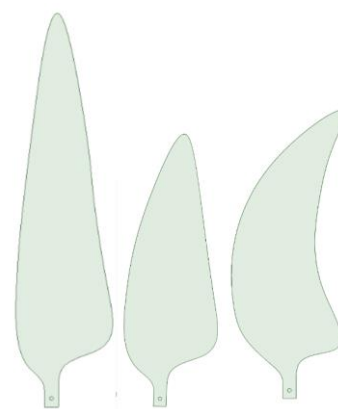


Figure 7: Various Flipper Designs

## Mechanical & Structural Design

All the internal components of the flapping mechanism, including the ball-and-socket joint, were very specific to this application. All the parts were 3D printed and therefore the objective was to reduce the mass of each component in order to minimize their printing costs. FEA or Finite Element Analysis was used on ANSYS Workbench 19 R1 to perform the structural analysis and optimize the design of these parts.

Instead of performing a dynamic analysis of the entire assembly, a conservative parts based static structural analysis was carried out to characterize the loads properly. A full dynamic analysis would have been very



complicated and hard to converge leading to the possibility of inaccurate results. Instead, loads and contacts were applied in a conservative manner to simulate the worst-case scenario for each component. This also negates the need for performing any fatigue analysis as a minimum factor of safety of 2 was chosen for each component. Topological optimization with a mass reduction objective function and yield stress as the stopping criterion was used to reduce the mass from the ideal areas [See appendix C].

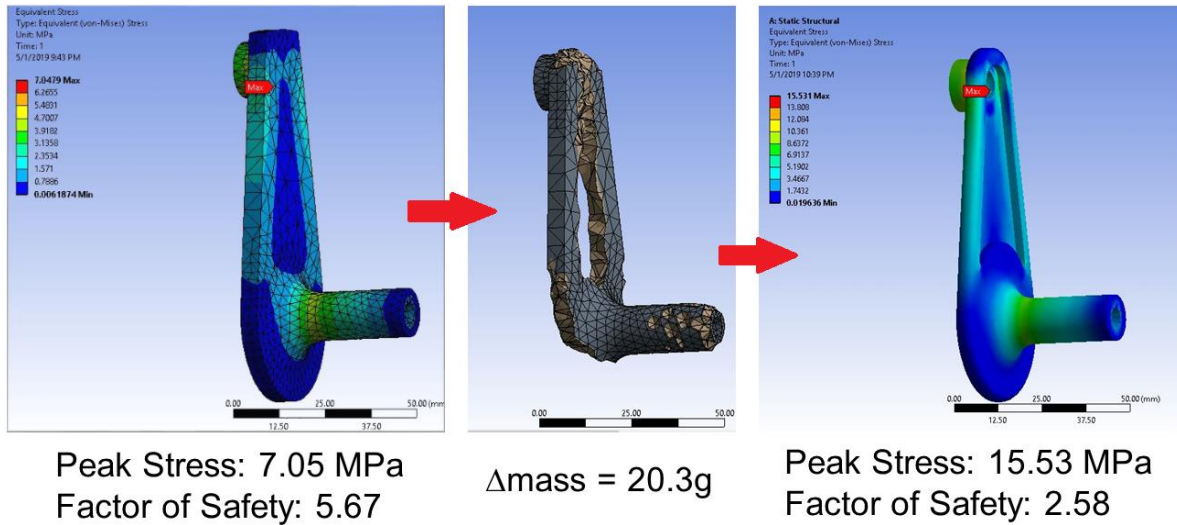


**Figure 8: Schematic of Topology Optimization and Stress Analysis**

## Hardware and Electronics

In order to incorporate two degrees of freedom on each flipper, enabling both the rolling and pitching motion, we spent a significant amount of time selecting our actuators and sensors. Our prototype required powerful, accurate and compact components to reduce overall volume and facilitate the sealing process. Acknowledging that all sensitive electrical components, except for the two waterproof servos, needed to be enclosed in an airtight box of finite dimensions to stay protected from water, the team designed and fabricated a custom PCB board which integrated all the necessary hardware. This layout led to a reduction in the overall volume of the electrical system and significantly improved its robustness by reducing the number of jumper wires required. It also enabled the accommodation of an internal power supply (LiPo battery) within the airtight box, obviating the need for a power tether. Figures 9 and 10 illustrate the schematic and board layout of the final PCB version respectively, as designed in Eagle 9.0 software.

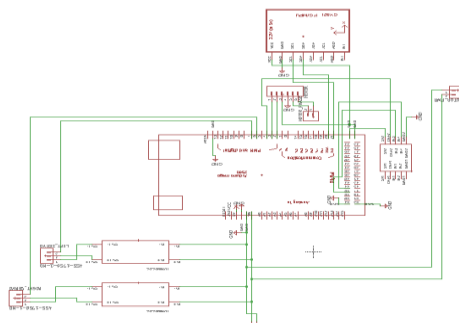


**Figure 9: Schematic layout of PCB**

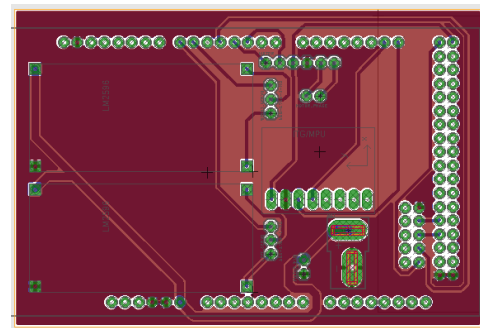


**Figure 10: Board layout of PCB**

The PID controller, running on the Arduino Mega MCU, drives the primary flapping motion by controlling the rotational velocity of the main motor, while the two servos control the pitch angle (along the axis of each flipper) to provide active cruise and orientation (roll) stability. The onboard IMU sensor outputs the necessary data to

balance the penguin when swimming while a temperature sensor monitors and notifies the users if the temperature inside the box rises above a certain threshold. This last feature is critical for the integrity of the sensitive electrical components and the LiPo battery contained in the sealed box. Figure 11 shows the complete electrical system independently, including all components and DC-DC converters for the servos, while Figure 12 shows the assembled system inside the airtight box on the rear part of the penguin's body.



**Figure 11: Complete electrical system**



**Figure 12: Assembled penguin's rear part**

### Body frame & Assembly

The mechanical design of the vehicle must integrate several subsystems. For the body frame, the main priorities of the construction were water tightness, hydrodynamics, and structural stability. The frame was constructed in two halves, which sealed at the center of the body with two O-rings bolted by eight bolts. From these two mating seals, a rib-and-spar structure was designed to take the outer shape of the body. Four spars run the length of the body forming a teardrop shape as determined by the computational fluid dynamics optimization and are at 45° from the horizontal plane. Eight ribs sit perpendicular to the spars and run at equal intervals for the length of the frame. These ribs and spars were laser cut from acrylic and tested using finite element analysis software to ensure that each component falls beneath yield stress. The ribs and spars mate with slots that were created such that the overall shape is more hydrodynamic. Additionally, the first and last ribs have connections for passive ballast to be placed to balance the center of mass while the third rib from the front incorporates a mate for the ball-and-socket joint. This overall shape maintains a structural integrity as tested in finite element analysis software while forming an optimized hydrodynamic shape.

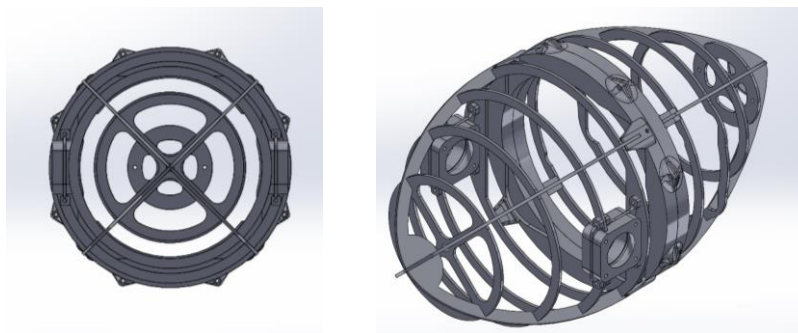


**Figure 13: Rib and spar structure of the frame**

The mating seal accounts for a watertight connection between the two halves. Two layers of waterproof material were placed around the outside of the penguin and sealed with epoxy at the central seals and wing sockets. The first material is a waterproof thermal-bonding polyurethane fabric that can seal with itself under high temperatures. The second layer was completed with an off-the-shelf rubber swimming cap for both halves of the penguin. This second layer is also sealed with epoxy to provide a more secure seal, while the edges of the swimming cap overlap to

provide extra support on top of the central seals. This outer shell acts as the first layer of water protection and encapsulates the two main elements of the penguin.

The front half of the penguin includes the flapping mechanism and waterproof servo motors, which sit inside the ribbed frame. The second half includes the non-waterproof and non-water-resistant elements including the central 131:1 DC motor, LiPo battery, and other electrical components. These water-susceptible components are housed within the second layer of protection, a watertight plastic container that connects with the external parts through the motor shaft, and two epoxy-sealed holes. The box sits in the stern of the penguin (behind the central seal), while the main flapping mechanism sits in the bow of the penguin frame. External connections which allow for some interaction (and possibilities of leaks) between the inner region within the rib-and-spar shell and the internal components include three areas. First, the rib design and custom bracket connects the ball-and-socket joint with the main flapping mechanism, which comprises the first two areas. The polyurethane thermally-bonding material mates with the outer edge of the joint allowing for flexibility while maintaining a waterproof connection. The third element that spans the gap to the external environment is the USB cable. This cable winds through an epoxy-sealed hole in the inner electronics box and through another epoxy-sealed hole in the two external waterproof layers to send and receive serial data.

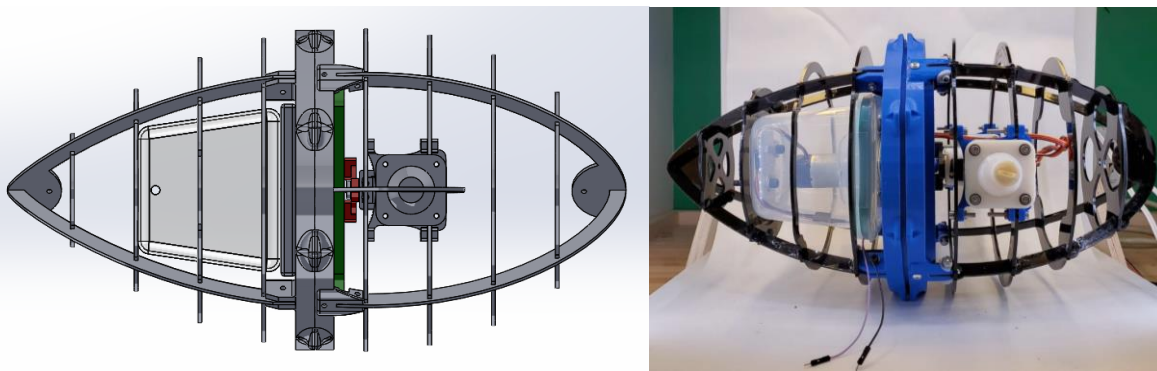


**Figure 14: Final CAD assembly (left) Actual Internal Structure (right)**

## Individual Technical Contributions

### Stam Athinotis

With coursework in Mechatronics, Controls and Kinematics, Stam focused on designing and fabricating the electronic system of the robot. He also implemented the control and system integration on the arduino microcontroller and designed the kinematic model of the mechanism.

### Angelos Mavrogiannis

With coursework in Kinematics, Dynamics and Computational Engineering, Angelos worked on the mechanical design using CAD software as well as on developing underwater simulations in Gazebo.

### William Moreno

With coursework in Applied Finite Element Analysis and Kinematics, Dynamic systems, and Controls, William focused on contributing to the mechanical design and kinematics of the penguin model. This included using ANSYS Mechanical to run Finite Element Analysis simulations and minimize certain properties using Topological Optimization.



## Pranav Narahari

With coursework in Kinematics, Dynamic systems, and Controls, Linear control systems and Multivariable linear controls, Pranav focussed on developing the kinematic and dynamic model and the controller of the robot. He designed the first mechanism and conducted kinematic analysis on all the mechanisms, contributed to the mechanism design and designed the PID controller for velocity control.

## Aniruddhan Unni

With coursework in Advanced Fluid Dynamics, Computational Fluid Dynamics and Applied FEA; Aniruddhan focused on doing the Mechanical Design, Stress Analysis and Hydrodynamic Design. This included CAD design and assembly on Solidworks, Structural FEA analysis and topological optimization on ANSYS Mechanical and CFD analysis on ANSYS Fluent.

## Experiments

Each subsystem of the robot was tested separately in order to ensure that everything worked as expected. Specifically, a custom test rig was laser cut from acrylic in order to mount and test the mechanism in its entirety, before fabricating the main body. Accordingly, the electronics and motors were tested on that, using different speeds and settings that would correspond to different propulsion scenarios and maneuvers. Our three-layer protection system from water was validated by performing a series of successful leak tests on each component that played a key role in each layer.

After building and assembling the body of the robot, multiple tests were conducted in order to assert the functionality of the mechanism under different values of input parameters. The robot was able to successfully perform a wide range of flapping motions (82 degrees) using the DC motor for the roll motion and the two servo motors for the pitch motion. A range of 20 - 120 rpm was fed to the motor and the complete range of the desired angle of attacks was achieved.

The final step of our testing process involved testing the robot in a water tank in order to validate the efficacy of our waterproofing system as well as our research hypothesis. Certain waterproofing and mechanism compliance issues were sorted out after the first test. The robot did not have an active ballast system and was very buoyant, necessitating the attachment of passive ballasts to keep it underwater. This was done by attaching a 7 kg mass and during the second test, where the production of thrust and forward propulsion was witnessed for a few seconds. However, a crucial part of our mechanism failed, and we were not able to conduct as many experiments as we had planned.

Using CFD simulations, the behaviour of the effect of higher aspect ratios and curved tips was observed to show that these features reduce the drag upto a certain point. This was attributed to the production of a smaller tip vortex with lower induced drag. This could have been verified with additional experimental data. The effect of wing flex couldn't be tested computationally as the resources to run large transient simulations with Fluid Structure Interactions were not available.

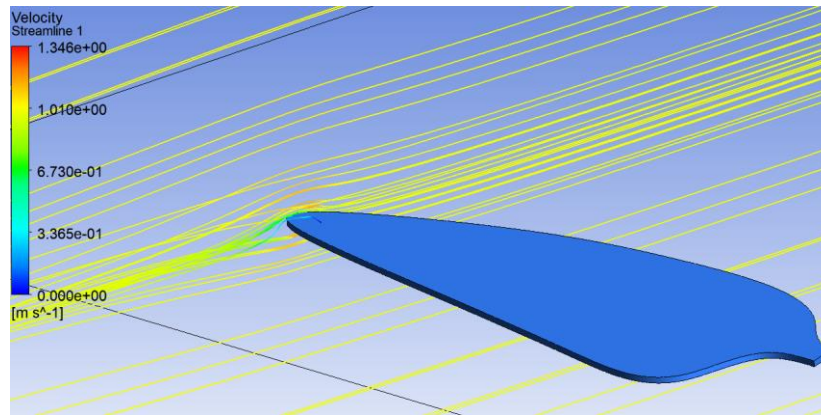


**Figure 14: Velocity streamlines illustrating the wing tip vortex**

## Stretch Goals

During the project, the mechanism underwent major changes due to which there was a delay in the development of the final prototype. Given this delay, only certain stretch goals were achieved:

1. Successful implementation of a passive tail (vertical/horizontal stabilizer) to aid pitch and yaw motion respectively.
2. Successful implementation of a ball-and-socket joint facilitating the addition of a third degree of freedom for the flippers to rotate the plane in which they flap.

Given additional time and resources to expand the project, the team would verify the research hypothesis experimentally by testing flippers of different size, shape and flexibility and quantifying the change in velocity and energy consumption. Given that the buoyancy of the robot was an issue, we would look into adding an active ballast system to ensure the robot is submerged underwater at all times. Moreover, given the potential of this platform, adding complete active stability/maneuverability controls along with autonomous capabilities would be the goal.

Finally, the current design had certain small issues with compliance, waterproofing and tolerances. These issues can be ameliorated by exploring simpler and more robust ways to manufacture the body of the robot and ensuring proper tolerancing of the 3D printed parts.

## Budget

Figure 16 illustrates our budget allocation for the project. The bar chart clearly shows that the majority of the budget was allocated on the fabrication of the body and the mechanism, which mainly consisted of 3D printed and laser cut parts. The total amount of money spent (\$850) was slightly over our planned and available budget (\$800), as we had not accounted for some unexpected expenses, such as shipping costs. However, we are currently returning some items that were not used and it is expected that the overall money spent after the refund is going to be \$815.



Figure 16: Budget Allocation

## References

- [1] “Robots in the World”, *Underwater Robots Advancing Marine Research* (2018)
- [2] Vartan S., “Why do we know more about the surface of Mars than we do about the ocean floor”, MNN, (2016), <https://www.mnn.com/earth-matters/wilderness-resources/blogs/why-do-we-know-more-about-surface-mars-we-do-about-ocean-floor>
- [3] Techet, Alexandra H. "Propulsive performance of biologically inspired flapping foils at high Reynolds numbers." *Journal of Experimental Biology* 211.2 (2008): 274-279.
- [4] Phillips et al., “Nature in engineering for monitoring the oceans: comparison of the energetic costs of marine animals and AUVs,” *Further Advances in Marine Unmanned Vehicles* (2012): 373 - 405
- [5] Clear Flight Solutions. “Robird: Methods.” *Robird*, Clear Flight Solutions (2018), [clearflightsolutions.com/methods/robirds](http://clearflightsolutions.com/methods/robirds).
- [6] NUS, “NUS-Developed Manta Ray Swims Faster and Operates Up to 10 Hours.” *NUS News* (2017), <http://news.nus.edu.sg/press-releases/NUS-robotic-manta-ray>
- [7] Festo, AG & Co., *AquaPenguins* (2009)
- [8] Yamaguchi, H., and N. Bose. "Oscillating foils for marine propulsion." *Oscillating Foils for Marine Propulsion* 3 (1994): 539-544.
- [9] Malik, M. Afzaal, and Farooq Ahmad. "Effect of different design parameters on lift, thrust, and drag of an ornithopter." *Proceedings of the world congress on engineering*. Vol. 2. 2010.
- [10] Rose, Cameron Jarrel. “Modeling and control of an ornithopter for non-equilibrium maneuvers”. Diss. UC Berkeley, 2015.
- [11] Lovvorn, J., et al. "Hydrodynamic drag of diving birds: effects of body size, body shape and feathers at steady speeds." *Journal of Experimental Biology* 204.9 (2001): 1547-1557.

## Appendix

### A.1 Mechanism python script-

```
import numpy as np
import matplotlib.pyplot as plt

def CalcPoints(d, l1, l2, phi, x0, y0):
    x = np.zeros(3)
    y = np.zeros(3)
    th1 = np.arcsin(d/l1)
    th2 = -(th1 + np.pi - phi)
    x[0] = x0
    y[0] = d + y0
    x[1] = x[0] + l1*np.cos(th1)
    y[1] = y0
    x[2] = x[1] + l2*np.cos(th2)
    y[2] = y[1] + l2*np.sin(th2)
    return x,y, th2*180//np.pi

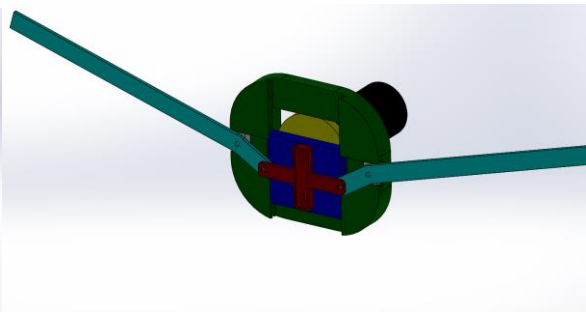
# Orientation Figure
plt.figure(figsize=(8,8))
# plt.axis([-0.04,0.04,-0.044,0.04])
plt.plot((0,0.04),(0,0), c = 'k') #Plot x axis
plt.plot((0,0),(-0.04,0.04), c = 'k') #Plot y axis
x0 = 0
y0 = 0
d = 0.019
l1 = 0.02
l2 = 0.02
phi = 170*np.pi/180
x,y,flip_angle = CalcPoints(d, l1, l2, phi, x0, y0)
circle = plt.Circle((x[1],y[1]),l2, color='g',fill=False)
plt.gcf().gca().add_artist(circle)

plt.title("Flipper Orientation")
plt.scatter(x,y, c = 'b')
plt.plot(x,y, c = 'b')
# plt.legend(flip_angle)

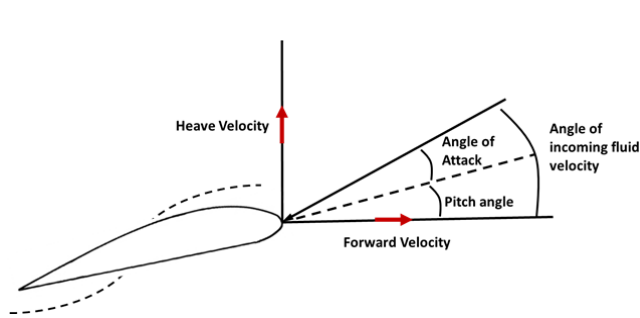
d = -d -0.0005
x,y,flip_angle1 = CalcPoints(d, l1, l2, phi, x0, y0)
# plt.scatter(x,y,color = 'r')
# plt.plot(x,y, c = 'r')
plt.scatter(x,y, c = 'r')
plt.plot(x,y, c = 'r')
plt.legend(["x axis", "y axis", flip_angle, flip_angle1])
plt.show()
```



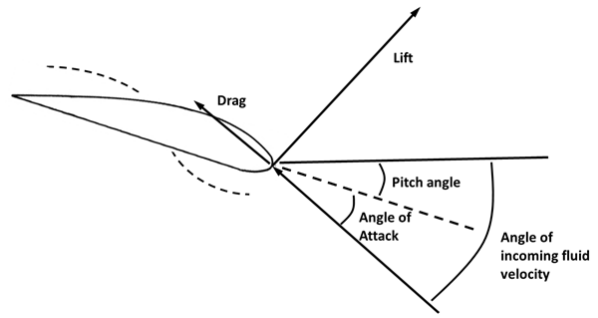
*Appendix A2: Dual wiper mechanism*



*Appendix A3: Final Flipper Mechanism Model*



*Appendix A4: Dynamic model*



*Appendix A5: Dynamic model*

## B.1 CFD Parameters

The bullet domain that was used extends 10 flipper lengths upstream, 20 flipper lengths upstream and 5 flipper lengths to the side. This was done to ensure that all the flow features were captured while keeping the domain size to a minimum.

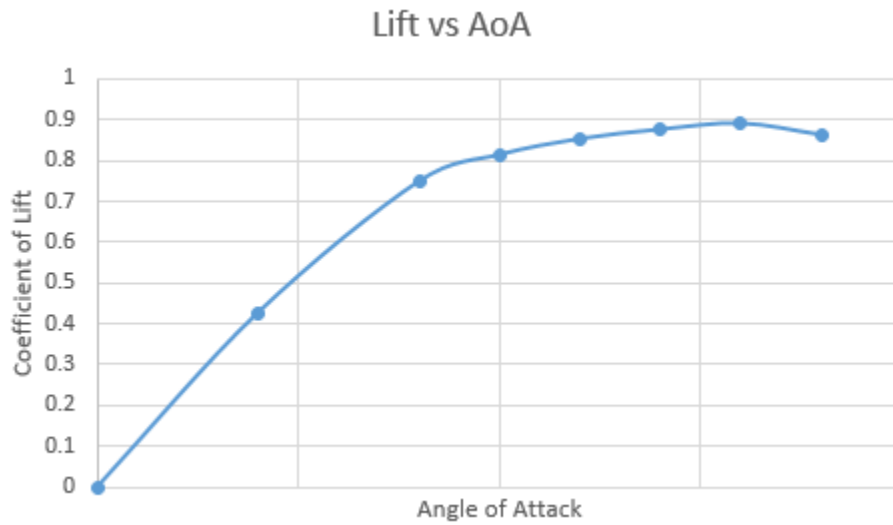
The tetrahedral mesher was used with an inflation mesh over the surface and surface refinements around the the base and tip of the flipper. The fine mesh was chosen based on the Grid Convergence Study shown below. The resultant average wall  $y^+$  value was close to 50.

Mesh	Number of Nodes	Element Size	Coefficient of Drag ( $C_d$ )
Coarse	95,000	50mm	0.521
Default	335,000	20mm (approx)	0.536
Fine	479,000	10mm	0.541
Very Fine	1,579,400	7mm	0.542

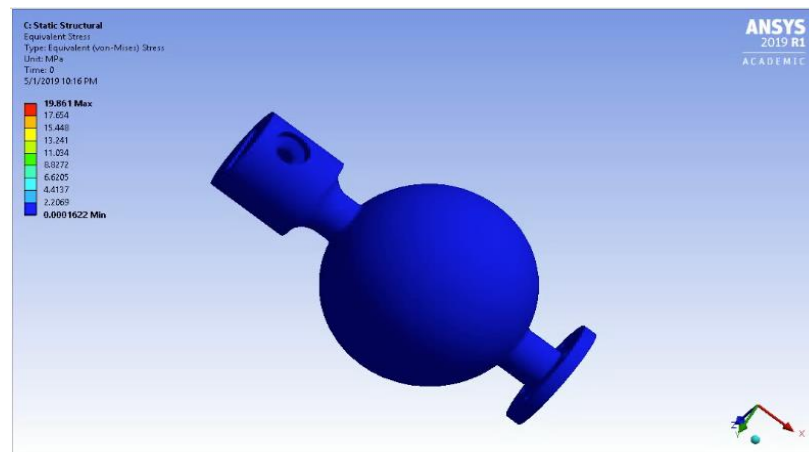
**Table B.2 Mesh Independence Studies for the Body Design Simulations**



## B2. Lift Curve for base flipper obtained from CFD



## C. FEA Analysis



Peak Stress: 19.86 MPa  
Yield Stress: 40 MPa  
Factor of Safety: 2.01

**Carnegie  
Mellon  
University**

Figure C.1: Ball Joint Stress Analysis

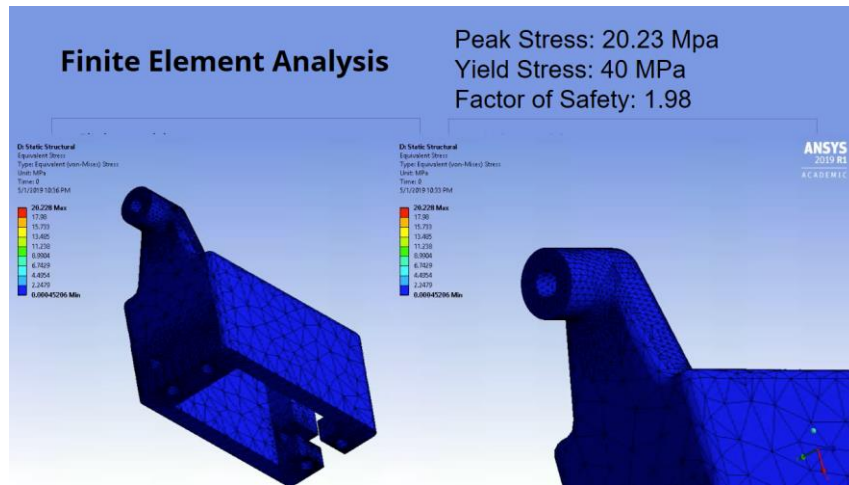


**Figure C.2: Servo Mount Stress Analysis**